

An Improved Bound on the Optimal Paper Moebius Band

Richard Evan Schwartz *

August 27, 2020

Abstract

We show that a smooth embedded paper Moebius band must have aspect ratio at least

$$\lambda_1 = \frac{2\sqrt{4 - 2\sqrt{3}} + 4}{\sqrt[4]{3}\sqrt{2} + 2\sqrt{2\sqrt{3} - 3}} = 1.69497\dots$$

This bound comes more than 3/4 of the way from the old known bound of $\pi/2 = 1.5708\dots$ to the conjectured bound of $\sqrt{3} = 1.732\dots$

1 Introduction

This paper addresses the following question. *What is the aspect ratio of the shortest smooth paper Moebius band?* Let's state the basic question more precisely. Given $\lambda > 0$, let

$$M_\lambda = ([0, 1] \times [0, \lambda]) / \sim, \quad (x, 0) \sim (1 - x, \lambda) \quad (1)$$

denote the standard flat Moebius band of width 1 and height λ . This Moebius band has aspect ratio λ . Let $S \subset \mathbf{R}_+$ denote the set of values of λ such that

*Supported by N.S.F. Grant DMS-1807320

there is a smooth ¹ isometric embedding $I : M_\lambda \rightarrow \mathbf{R}^3$. The question above asks for the quantity

$$\lambda_0 = \inf S. \tag{2}$$

The best known result, due to Halpern and Weaver [HW], is that

$$\lambda_0 \in [\pi/2, \sqrt{3}]. \tag{3}$$

In §14 of their book, *Mathematical Omnibus* [FT], Fuchs and Tabachnikov give a beautiful exposition of the problems and these bounds. This is where I learned about the problem.

The lower bound is local in nature and does not see the difference between immersions and embeddings. Indeed, in [FT], a sequence of immersed examples whose aspect ratio tends to $\pi/2$ is given. The upper bound comes from an explicit construction. The left side of Figure 1.1 shows $M_{\sqrt{3}}$, together with a certain union of *bends* drawn on it. The right side shows the nearly embedded paper Moebius band one gets by folding this paper model up according to the bending lines.

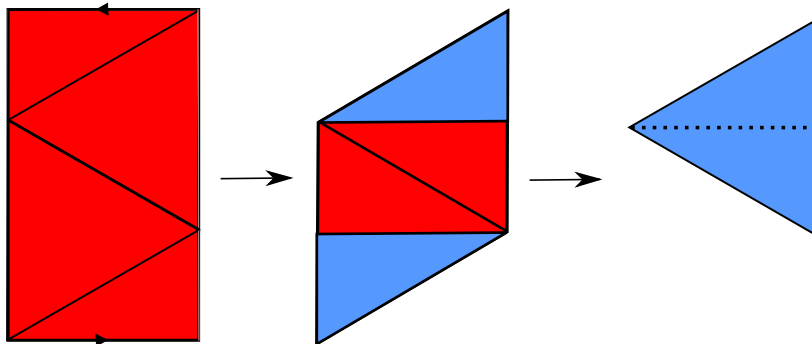


Figure 1.1: The conjectured optimal paper Moebius band

The Moebius band just described is degenerate: It coincides as a set with the equilateral triangle Δ of semi-perimeter $\sqrt{3}$. However, one can choose any $\epsilon > 0$ and find a nearby smoothly embedded image of $M_{\sqrt{3}+\epsilon}$ by a process

¹ The smoothness requirement (or some suitable variant) is necessary in order to have a nontrivial problem. Given any $\epsilon > 0$, one can start with the strip $[0, 1] \times [0, \epsilon]$ and first fold it (across vertical folds) so that it becomes, say, an $(\epsilon/100) \times \epsilon$ “accordion”. One can then easily twist this “accordion” once around in space so that it makes a Moebius band. The corresponding map from M_ϵ is an isometry but it cannot be approximated by smooth isometric embeddings.

of rounding out the folds and slightly separating the sheets. Halpern and Weaver conjecture that $\lambda_0 = \sqrt{3}$, so that the triangular example is the best one can do.

The Moebius band question in a sense goes back a long time, and it is related to many topics. The early paper [Sa] proves rigorously that smooth paper Moebius bands exist. (See [HF] for a modern translation to english.) The paper [CF] gives a general framework for considering the differential geometry of developable surfaces. Some authors have discussed optimal shapes for Moebius bands from other perspectives, e.g. algebraic or physical. See, e.g. [MK] and [S1]. The Moebius band question has connections to origami. See e.g. the beautiful examples of isometrically embedded flat tori [AHLM]. It is also related to the main optimization question from geometric knot theory: What is the shortest piece rope one can use to tie a given knot? See e.g. [CKS]. Finally (as we discuss in §5) the Moebius band question related to topics in discrete computational geometry such as tensegrities [CB].

In this paper we improve the lower bound.

Theorem 1.1 (Main) *An embedded paper Moebius band must have aspect ratio at least*

$$\lambda_1 = \frac{2\sqrt{4 - 2\sqrt{3}} + 4}{\sqrt[4]{3}\sqrt{2} + 2\sqrt{2\sqrt{3} - 3}} = 1.69497\dots$$

This value λ_1 arises naturally in a geometric optimization problem involving trapezoids. To quantify the way that our result improves over the previous lower bound, we note that $\lambda_1 > \sqrt{3} - (1/26)$ whereas $\pi/2 < \sqrt{3} - (4/26)$.

The proof of the Main Theorem has 2 ideas, which we now explain. Being a ruled surface, $I(M_\lambda)$ contains a continuous family of line segments which have their endpoints on $\partial I(M_\lambda)$. We call these line segments *bend images*. Say that a *T-pattern* is a pair of perpendicular coplanar bend images. The *T-pattern* looks somewhat like the two vertical and horizontal segments on the right side of Figure 1.1 except that the two segments are disjoint in an embedded example. Here is our first idea.

Lemma 1.2 *An embedded paper Moebius band of aspect ratio less than $7\pi/12$ contains a T-pattern.*

Note that $7\pi/12 > \sqrt{3}$, so Lemma 1.2 applies to the examples of interest to us. Lemma 1.2 relies crucially on the embedding property. The immersed examples in [FT] do not have these *T-patterns*.

The two bend images comprising the T -pattern divide $I(M)$ into two halves. Our second idea is to observe that the image $I(\partial M_\lambda)$ makes a loop which hits all the vertices of the T -pattern. When we compare the relevant portions of ∂M_λ with a polygon made from the vertices of the T -pattern, we get two constraints which lead naturally to the lower bound of λ_1 .

Since we can almost effortlessly give *some* improvement to the lower bound using Lemma 1.2, we do this now. The convex hull of the T -pattern contains a triangle of base at least 1 and height at least 1. Such a triangle has semi-perimeter at least $\phi = 1.61\dots$, the golden ratio. Hence $\lambda_0 \geq \phi$. The argument which gives $\lambda_0 \geq \lambda_1$, the constant in Theorem 1.1, is similar in spirit but more elaborate.

It would have been nice if the existence of a T -pattern forced $\lambda > \sqrt{3}$ on its own. This is not the case. In Figure 2.1 we show half of an immersed paper Moebius band of aspect ratio less than $\sqrt{3}$ that has a T -pattern. I did not try to formally prove that these exist, but using my computer program I can construct them easily. I will sketch a finite dimensional calculation which, if completed, would show that an immersed paper Moebius band with a T -pattern has aspect ratio at least $\sqrt{3} - (1/58) = 1.7148\dots$ This would significantly improve the bound in Theorem 1.1, but I don't know how to make the calculation feasible.

This paper is organized as follows. In §2 we introduce some basic geometric objects associated to a paper Moebius band and then prove Lemma 1.2. In §3 we give the argument involving the vertices of the T -pattern and thereby prove Theorem 1.1. In §4 we prove Theorem 4.1, a result which refines Theorem 1.1 in some sense. In §5 we discuss the (infeasible) calculation mentioned above and briefly indulge in some speculation about how these kinds of calculations could possibly show that $\lambda_0 \geq \sqrt{3}$. The brief nature of the speculation belies the enormous amount of time I spent trying to make this work. I am still trying.

I would like to thank Sergei Tabachnikov for telling me about this problem and for helpful discussions about it. I would also like to thank the Simons Foundation and the Institute for Advanced Study for their support during my 2020-21 sabbatical.

2 Existence of the T Pattern

2.1 Polygonal Moebius Bands

Basic Definition: Say that a *polygonal Moebius band* is a pair $\mathcal{M} = (\lambda, I)$ where $I : M_\lambda \rightarrow \mathbf{R}^3$ is an isometric embedding that is affine on each triangle of a triangulation of M_λ . We insist that the vertices of these triangles all lie on ∂M_λ , as in Figure 1.1. Any smooth isometric embedding $I' : M_\lambda \rightarrow \mathbf{R}^3$ can be approximated arbitrarily closely by this kind of map, so it suffices to work entirely with polygonal Moebius bands.

Associated Objects: Let $\delta_1, \dots, \delta_n$ be the successive triangles of \mathcal{M} .

- The *ridge* of δ_i is edge of δ_i that is contained in ∂M_λ .
- The *apex* of δ_i to be the vertex of δ_i opposite the ridge.
- A *bend* is a line segment of δ_i connecting the apex to a ridge point.
- A *bend image* is the image of a bend under I .
- A *facet* is the image of some δ_i under I .

We always represent M_λ as a parallelogram with top and bottom sides identified. We do this by cutting M_λ open at a bend. See Figure 2.1 below.

The Sign Sequence: Let $\delta_1, \dots, \delta_n$ be the triangles of the triangulation associated to \mathcal{M} , going from bottom to top in P_λ . We define $\mu_i = -1$ if δ_i has its ridge on the left edge of P_λ and $+1$ if the ridge is on the right. The sequence for the example in Figure 1.1 is $+1, -1, +1, -1$.

The Core Curve: There is a circle γ in M_λ which stays parallel to the boundary and exactly $1/2$ units away. In Equation 1, this circle is the image of $\{1/2\} \times [0, \lambda]$ under the quotient map. We call $I(\gamma)$ the *core curve*.

The left side of Figure 2.1 shows M_λ and the pattern of bends. The vertical white segment is the bottom half of γ . The right side of Figure 2.1 (which has been magnified to show it better) shows $I(\tau)$ where τ is the colored half of M_λ . All bend angles are π and the whole picture is planar. The colored curve on the right is the corresponding half of the core curve. Incidentally, for τ we have $L + R = 1.72121\dots < \sqrt{3}$.

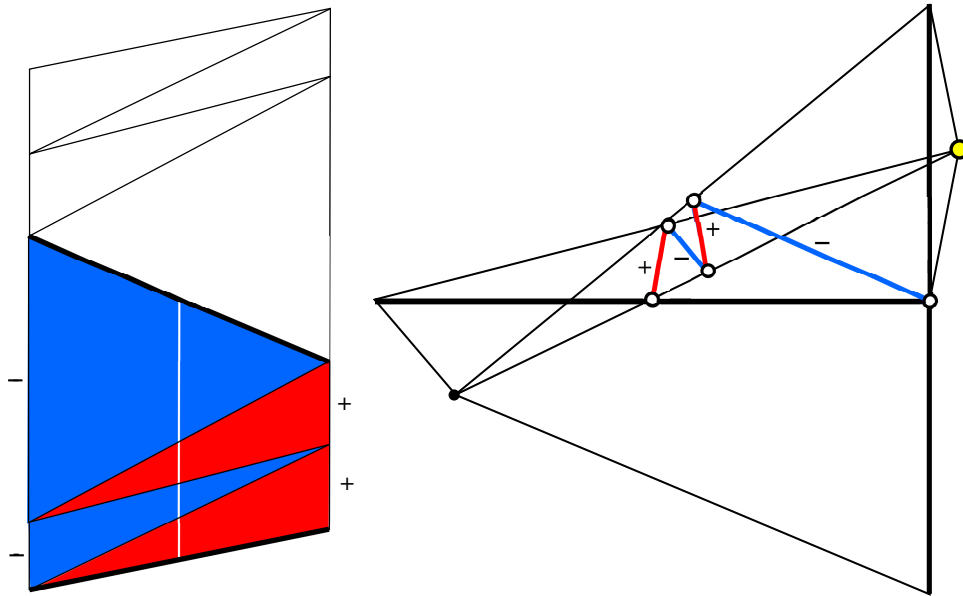


Figure 2.1: The bend pattern and the bottom half of the image

The Ridge Curve: We show the picture first, then explain.

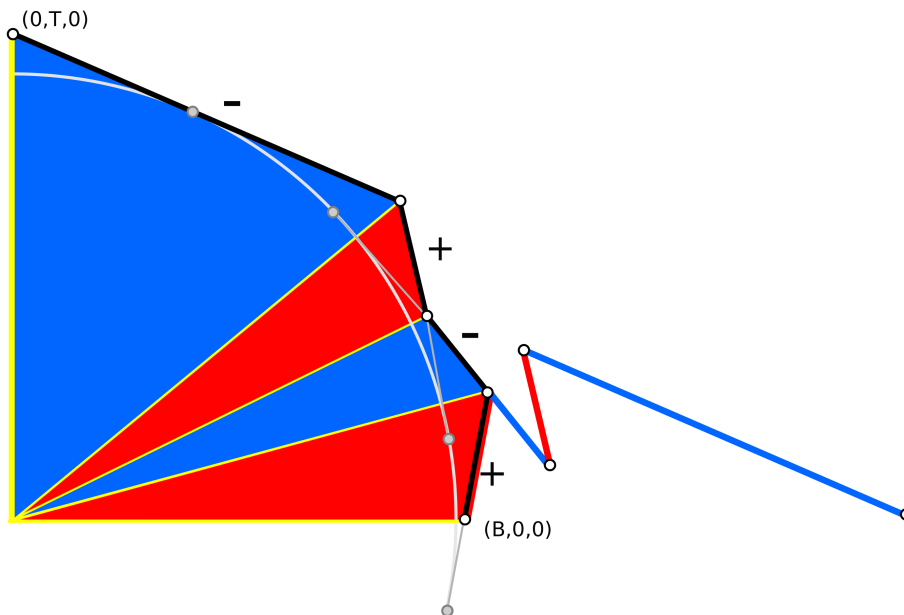


Figure 2.2: Half 2x core curve (red/blue) and half ridge curve (black).

Let β_b be the bottom edge of the parallelogram representing M_λ . We normalize so that I maps the left vertex of β_b to $(0, 0, 0)$ and the right vertex to $(B, 0, 0)$, where B is the length of β_b . Let E_1, \dots, E_n be the successive edges of the core curve, treated as vectors. Let

$$\Gamma'_i = 2\mu_i E_i, \quad i = 1, \dots, n. \quad (4)$$

Let Γ be the curve whose initial vertex is $(B, 0, 0)$ and whose edges are $\Gamma'_1, \dots, \Gamma'_n$. Here μ_1, \dots, μ_n is the sign sequence.

Γ has length 2λ , connects $(B, 0, 0)$ to $(-B, 0, 0)$, and is disjoint from the open unit ball. The lines extending the sides of Γ are tangent to the unit sphere. We rotate so that Γ contains $(0, T, 0)$ for some $T > 1$. If we cone Γ to the origin, we get a collection $\Delta_1, \dots, \Delta_n$ of triangles, and Δ_i is the translate of $\mu_i I(\delta_i)$ whose apex is at the origin. In particular, the vectors pointing to the vertices of Γ are parallel to the corresponding bend images. Figure 2.2 shows the portion of the ridge curve (in black) associated to the example in Figure 2.1. We have also scaled the core curve by 2 and translated it to show the relationships between the two curves.

2.2 Geometric Bounds

While we are in the neighborhood, we re-prove the lower bound from [FT]. The proof in [FT] is somewhat similar, though it does not use the ridge curve. Let λ be the aspect of the polygonal Moebius band \mathcal{M} and let Γ be the associated ridge curve. Let $f : \mathbf{R}^3 - B^3 \rightarrow S^2$ be orthogonal projection. The map f is arc-length decreasing. Letting $\Gamma^* = f(\Gamma)$, we have $|\Gamma^*| < |\Gamma| = 2\lambda$. Since Γ^* connects a point on S^2 to its antipode, $|\Gamma^*| \geq \pi$. Hence $\lambda > \pi/2$.

Now we use the same idea in a different way.

Lemma 2.1 *Suppose \mathcal{M} has aspect ratio less than $7\pi/12$. Then the ridge curve Γ lies in the open slab bounded by the planes $Z = \pm 1/\sqrt{2}$.*

Proof: We divide Γ into halves. One half goes from $(B, 0, 0)$ to $(0, T, 0)$ and the second half goes from $(0, T, 0)$ to $(-B, 0, 0)$. Call the first half Γ_1 . Suppose that Γ_1 intersects the plane $Z = 1/\sqrt{2}$. Then the spherical projection Γ_1^* goes from $A = (1, 0, 0)$ to some unit vector $B = (u, v, 1/\sqrt{2})$ to $C = (0, 1, 0)$. Here $u^2 + v^2 = 1/2$. The shortest path like this is the geodesic bigon connecting A to B to C . Such a bigon has length at least

$$\arccos(A \cdot B) + \arccos(B \cdot C) = \arccos(u) + \arccos(v) \geq^* 2 \arccos(1/2) = 2\pi/3.$$

The starred inequality comes from the fact that the minimum, subject to the constraint $u^2 + v^2 = 1/2$, occurs at $u = v = 1/2$.

But then Γ has length at least $2\pi/3 + \pi/2 = 7\pi/6$. This exceeds twice the aspect ratio of \mathcal{M} . This is a contradiction. The same argument works if Γ_1 hits the plane $Z = -1/\sqrt{2}$. Likewise the same argument works with the second half of Γ in place of the first half. ♠

Corollary 2.2 *Suppose \mathcal{M} has aspect ratio less than $7\pi/12$. Let β_1^* and β_2^* be two perpendicular bend images. Then a plane parallel to both β_1^* and β_2^* cannot contain a vertical line.*

Proof: Every bend image is parallel to some vector from the origin to a point of Γ . By the previous result, such a vector make an angle of less than $\pi/4$ with the XY -plane. Hence, all bend images make angles of less than $\pi/4$ with the XY -plane. Suppose our claim is false. Since β_1^* and β_2^* are perpendicular to each other, one of them must make an angle of at least $\pi/4$ with the XY -plane. This is a contradiction. ♠

2.3 Perpendicular Lines

As a prelude to the work in the next section, we prove a few results about lines and planes. Say that an *anchored line* in \mathbf{R}^3 is a line through the origin. Let Π_1 and Π_2 be planes through the origin in \mathbf{R}^3 .

Lemma 2.3 *Suppose that Π_1 and Π_2 are not perpendicular. The set of perpendicular anchored lines (L_1, L_2) with $L_j \in \Pi_j$ for $j = 1, 2$ is diffeomorphic to a circle.*

Proof: For each anchored line $L_1 \in \Pi_1$ the line $L_2 = L_1^\perp \cap \Pi_2$ is the unique choice anchored line in Π_2 which is perpendicular to L_1 . The line L_2 is a smooth function of L_1 . So, the map $(L_1, L_2) \rightarrow L_1$ gives a diffeomorphism between the space of interest to us and a circle. ♠

A *sector* of the plane Π_j is a set linearly equivalent to the union of the $(++)$ and $(--)$ quadrants in \mathbf{R}^2 . Let $\Sigma_j \subset \Pi_j$ be a sector. The boundary $\partial\Sigma_j$ is a union of two anchored lines.

Lemma 2.4 *Suppose (again) that the planes Π_1 and Π_2 are not perpendicular. Suppose also that no line of $\partial\Sigma_1$ is perpendicular to a line of $\partial\Sigma_2$. Then the set of perpendicular pairs of anchored lines (L_1, L_2) with $L_j \in \Sigma_j$ for $j = 1, 2$ is either empty or diffeomorphic to a closed line segment.*

Proof: Let S^1 denote the set of perpendicular pairs as in Lemma 2.3. Let $X \subset S^1$ denote the set of those pairs with $L_j \in \Sigma_j$. Let π_1 and π_2 be the two diffeomorphisms from Lemma 2.3. The set of anchored lines in Σ_j is a line segment and hence so is its inverse image $X_j \subset S^1$ under π_j . We have $X = X_1 \cap X_2$. Suppose X is nonempty. Then some $p \in X$ corresponds to a pair of lines (L_1, L_2) with at most one $L_j \in \partial\Sigma_j$. But then we can perturb p slightly, in at least one direction, so that the corresponding pair of lines remains in $\Sigma_1 \times \Sigma_2$. This shows that $X_1 \cap X_2$, if nonempty, contains more than one point. But then the only possibility, given that both X_1 and X_2 are segments, is that their intersection is also a segment. ♠

2.4 The Space of Perpendicular Pairs

We prove the results in this section more generally for piecewise affine maps $I : M_\lambda \rightarrow \mathbf{R}^3$ which are not necessarily local isometries. The reason for the added generality is that it is easier to make perturbations within this category. Let \mathbf{X} be the space of such maps which also satisfy the conclusion of Corollary 2.2. (In this section we will not use this property but in the next section we will.) So, \mathbf{X} includes all (isometric) polygonal Moebius bands of aspect ratio less than $7\pi/12$. The notions of bend images and facets makes sense for members of \mathbf{X} .

Lemma 2.5 *The space \mathbf{X} has a dense set \mathbf{Y} which consists of members such that no two facets lie in perpendicular planes and no two special bend images are perpendicular.*

Proof: One can start with any member of \mathbf{X} and postcompose the whole map with a linear transformation arbitrarily close to the identity so as to get a member of \mathbf{Y} . The point is that we just need to destroy finitely many perpendicularity relations. ♠

Let γ be center circle of M_λ . We can identify the space of bend images of \mathcal{M} with γ : The bends and bend-images are in bijection, and each bend intersects γ once. The space of ordered pairs of unequal bend images can be identified with $\gamma \times \gamma$ minus the diagonal. We compactify this space by adding in 2 boundary components. One of the boundary components comes from approaching the main diagonal from one side and the other comes from approaching the diagonal from the other side. The resulting space A is an annulus. For the rest of the section we choose a member of \mathbf{Y} and make all definitions for this member.

Lemma 2.6 \mathcal{P} is a piecewise smooth 1-manifold in A .

Proof: We apply Lemma 2.4 to the planes through the origin parallel to the facets and to the anchored lines parallel to the bend images within the facets. (Within a single facet the bend images and the corresponding anchored lines are in smooth bijection.) By Lemma 2.4, the space \mathcal{P} is the union of finitely many smooth connected arcs. Each arc corresponds to an ordered pair of facets which contains at least one point of \mathcal{P} . Each of these arcs has two endpoints. Each endpoint has the form (β_1^*, β_2^*) where exactly one of these bend images is special. Let us say that β_1^* is special. Then β_1^* is the edge between two consecutive facets, and hence (β_1^*, β_2^*) is the endpoint of exactly 2 of the arcs. Hence the arcs fit together to make a piecewise smooth 1-manifold. ♠

A component of \mathcal{P} is *essential* if it separates the boundary components of A .

Lemma 2.7 \mathcal{P} has an odd number of essential components.

Proof: An essential component, being embedded, must represent a generator for the first homology $H_1(A) = \mathbf{Z}$. By duality, a transverse arc running from one boundary component of A to the other intersects an essential component an odd number of times and an inessential component an even number of times. Let a be such an arc. As we move along a the angle between the corresponding bends can be chosen continuously so that it starts at 0 and ends at π . Therefore, a intersects \mathcal{P} an odd number of times. But this means that there must be an odd number of essential components of \mathcal{P} . ♠

2.5 The Main Argument

Now we prove Lemma 1.2. Say that a member of \mathbf{X} is *good* if (with respect to this member) there is a path connected subset $\mathcal{K} \subset \mathcal{P}$ such that both (β_1^*, β_2^*) and (β_2^*, β_1^*) belong to \mathcal{K} for some pair (β_1^*, β_2^*) .

Lemma 2.8 *If \mathcal{M} is good then \mathcal{M} has a T -pattern.*

Proof: Each pair (β_1^*, β_2^*) in \mathcal{P} determines a unique pair of parallel planes (P_1, P_2) such that $\beta_j^* \subset P_j$ for $j = 1, 2$. By hypothesis, members These planes do not contain vertical lines. Hence, our planes intersect the Z -axis in single and continuously varying points. As we move along \mathcal{K} these planes exchange places and so do their Z -intercepts. So, at some instant, the planes coincide and give us a T -pattern. ♠

Lemma 2.9 *A dense set of members of \mathbf{X} are good.*

Proof: Let \mathbf{Y} be the dense subset of \mathbf{X} considered in the previous section. Relative to any member of \mathbf{Y} , the space \mathcal{P} is a piecewise smooth 1-manifold of the annulus A with an odd number of essential components. The involution ι , given by $\iota(p_1, p_2) = (p_2, p_1)$, is a continuous involution of A which preserves \mathcal{P} and permutes the essential components. Since there are an odd number of these, ι preserves some essential component of \mathcal{P} . But then this essential component contains our set \mathcal{K} . ♠

Now we know that there are T -patterns for members of a dense subset of \mathbf{X} . By compactness and continuity, every member of \mathbf{X} has a T -pattern. By Corollary 2.2, \mathbf{X} contains all (ordinary) embedded polygonal Moebius bands of aspect ratio less than $7\pi/12$. Hence all such embedded Moebius bands contain T -patterns. This completes the proof of Lemma 1.2.

3 The Aspect Ratio Bound

3.1 Constraints coming from the T Pattern

Let \mathcal{M} be a polygonal Moebius band of aspect ratio $\lambda < 7\pi/12$. We keep the notation from the previous chapter.

Let β_1 and β_2 be two bends whose corresponding images $\beta_1^* = I(\beta_1)$ and $\beta_2^* = I(\beta_2)$ form a T -pattern. Since these segments do not intersect, we can label so that the line extending β_2^* does not intersect β_1^* . We cut M_λ open along β_1 and treat β_1 as the bottom edge. We now set $\beta_b = \beta_1$ and $\beta_t = \beta_2$ and (re)normalize as in §2.1. So, β_b^* connects $(0, 0, 0)$ to $(B, 0, 0)$, and β_t^* is a translate of the segment connecting $(0, 0, 0)$ to $(0, T, 0)$. Here B and T are the lengths of these segments.

The left side of Figure 3.1 shows M_λ . Reflecting in a vertical line, we normalize so that $L_1 \geq R_1$. This means that $L_2 \geq R_2$. The right side of Figure 3.1 shows that T pattern, and the corresponding images of the sets on the left under the isometry I . The wiggly curves we have drawn do not necessarily lie in the XY -plane but their endpoints do.

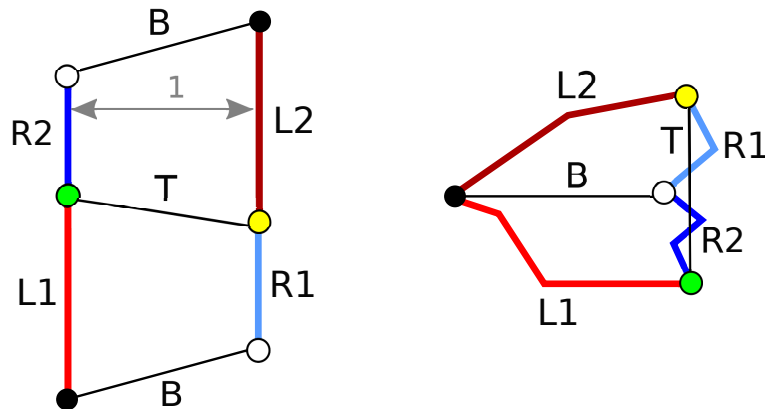


Figure 3.1: A Paper Moebius band interacting with the T -pattern.

There is some ϵ such that the distance from the white vertex to the yellow vertex is $T/2 + \epsilon$ and the distance from the white vertex to the yellow vertex is $T/2 - \epsilon$. Looking at the picture, and using the fact that geodesics in the Euclidean plane are straight lines, we get the following constraints:

$$R_1 + R_1 \geq T, \tag{5}$$

$$L_1 + L_2 \geq \sqrt{B^2 + (T/2 - \epsilon)^2} + \sqrt{B^2 + (T/2 + \epsilon)^2} \geq 2\sqrt{B^2 + T^2/4}. \tag{6}$$

3.2 An Optimization Problem

We are done with the Moebius band. We just have a parallelogram as on the left side of Figure 3.1 which satisfies the constraints in Equations 5 and 6 and we want to minimize $L_1 + L_2 + R_1 + R_2$. Let $L = (L_1 + L_2)/2$ and $R = (R_1 + R_2)/2$. If we replace L_1, L_2 by L, L and R_1, R_2 by R, R the constraints are still satisfied and the sum of interest is unchanged. The constraints now become:

$$2R \geq T, \quad L \geq \sqrt{B^2 + T^2/4}. \quad (7)$$

We show that $L + R \geq \lambda_1$, the constant from the Main Theorem, which means

$$\lambda = \frac{1}{2}(L_1 + L_2 + R_1 + R_2) = L + R \geq \lambda_1.$$

So, showing that $L + R \geq \lambda_1$ finishes the proof of the Main Theorem.

Let b and t respectively denote the slopes of the sides labeled B and T in Figure 3.2. Let $S = L + R$. Since $L \geq R$ we have $b \geq t$. In Figure 3.2 we depict the case when $b > 0$ and $t < 0$. As we see in the next section, this must happen when $S < \sqrt{3}$.

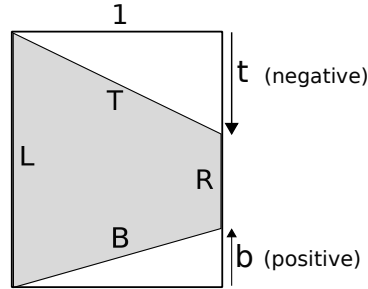


Figure 3.2: The basic trapezoid.

Since $L + R = S$ and $L - R = b - t$, and by the Pythagorean Theorem,

$$L = \frac{S + b - t}{2}, \quad R = \frac{S - b + t}{2}, \quad B = \sqrt{1 + b^2}, \quad T = \sqrt{1 + t^2}. \quad (8)$$

Plugging these relations into Equation 7, we get $S \geq f(b, t)$ and $S \geq g(b, t)$ where

$$f(b, t) = b - t + T, \quad g(b, t) = -b + t + \sqrt{4B^2 + T^2}.$$

Let $\phi = \max(f, g)$ and let D be the domain where $b \geq t$. We have $S \geq \phi$. To finish the proof of the Main Theorem we just need to show that $\min_D \phi = \lambda_1$. This is what we do.

Lemma 3.1 ϕ achieves its minimum at a point in the interior of D , and at this point we have $f = g$.

Proof: We note 3 properties of our functions:

1. $f(0, -1/\sqrt{3}) = g(0, -1/\sqrt{3}) = \sqrt{3}$. Hence $\phi(0, -1/\sqrt{3}) = \sqrt{3}$.
2. On ∂D we have $g(b, b) = B\sqrt{5} \geq \sqrt{5}$. Hence $\min_{\partial D} \phi > \sqrt{3}$.
3. As $b^2 + t^2 \rightarrow \infty$ in D , we have $f, g \rightarrow +\infty$.

From these properties, we see that the global minimum of ϕ is achieved at some point in the interior of D . Next, we compute

$$\frac{\partial f}{\partial t} = -1 + \frac{t}{T} < 0, \quad \frac{\partial g}{\partial t} = 1 + \frac{t}{4B^2 + T^2} > 0.$$

Hence the gradients of f and g are never zero, and are never positive multiples of each other. For this reason, any point where ϕ achieves a global minimum lies on the set where $f = g$. ♠

Setting $f = g$ and solving for b , we get

$$b = \beta(t) = \frac{t^3 - T^3 - 3t}{3t^2 - 1}. \quad (9)$$

There no solutions to $f = g$ when $t = +1\sqrt{3}$ and Item 1 above (or a direct calculation) shows that $\beta(-1/\sqrt{3}) = 0$. In particular, β has a removable singularity at $t = -1/\sqrt{3}$ and hence is smooth on the domain

$$D^* = (-\infty, 1/\sqrt{3}).$$

When $t > 1/\sqrt{3}$ we have $b = \beta(t) < 0 < t$. Hence, only $t \in D^*$ corresponds to points in D . So, we just need show $\min_{D^*} \phi^* = \lambda_1$, where

$$\phi^*(t) = f(\beta(t), t) = \frac{2T(t^2 - tT - 1)}{3t^2 - 1} \quad (10)$$

As $t \rightarrow -\infty$ or $t \rightarrow 1/\sqrt{3}$ we have $\phi^*(t) \rightarrow +\infty$. Hence ϕ^* achieves its minimum on D^* at some point where $d\phi^*/dt = 0$. This happens only at

$$t_0 = -\sqrt{\frac{2}{\sqrt{3}}} - 1 = -.39332\dots$$

We check that $\phi^*(t_0) = \lambda_1$.

4 Further Results

4.1 A Refinement

Because we do not want to make potentially vacuous statements, we state all our results for immersed paper Moebius bands of aspect ratio less than $\sqrt{3}$. Thanks to Lemma 1.2, these results apply to any embedded examples, should they exist.

Referring to Figure 3.1, let $S_j = L_j + R_j$ for $j = 1, 2$. The aspect ratio of our paper Moebius band is $\lambda = (S_1 + S_2)/2$. Theorem 1.1 says that

$$\frac{S_1 + S_2}{2} \geq 1.69497\dots \approx \sqrt{3} - \frac{1}{27}.$$

Now we give a bound on each sum S_j separately. Our bound is just slightly weaker than the one in Theorem 1.1, but on the other hand it gives much more information.

Theorem 4.1 *For any immersed paper Moebius with a T -pattern and aspect ratio less than $\sqrt{3}$, we have $S_j \geq \sqrt{3} - \frac{1}{3}b(1 - 2b)$. In particular $S_j \geq \sqrt{3} - \frac{1}{24}$.*

The function $f(b) = \frac{1}{3}b(1 - 2b)$ is a quadratic function vanishes at $b = 0$ and $b = 1/2$ and has a maximum value of $1/24$. We found this function by trial and error. The rest of the chapter is devoted to proving Theorem 4.1, though we will mention some other results along the way.

4.2 The Range of Slopes

We continue with the notation from the previous chapter. In particular, let f and g be the two constraint functions from §3.2 and let $\phi = \max(f, g)$. Let Ω be the set of values (b, t) satisfying $\phi(b, t) < \sqrt{3}$. We plot Ω in Figure 4.1. These are the possible values (b, t) of slopes of bends which can participate in a T -pattern when the aspect ratio is less than $\sqrt{3}$.

We have added in some points and lines to help frame Ω , and in particular we have placed it inside a trapezoid which tightly hugs it. All the lines drawn touch $\partial\Omega$ except the red one, which lies just barely above Ω . The lines of slope $2/3$ and $4/3$ through $(0, -1/\sqrt{3})$ are tangent to Ω . The right vertex of Ω is $(a, -a/2)$ where $a = (\sqrt{27} - \sqrt{11})/4$.

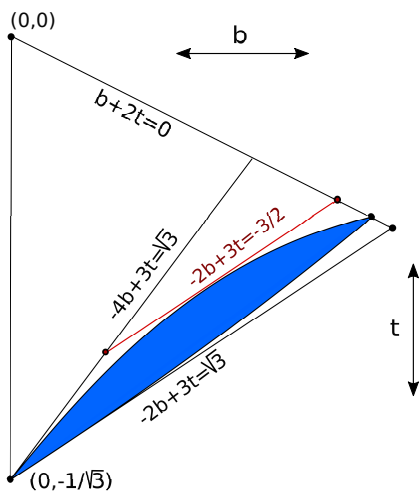


Figure 4.1: The range of slopes.

Some routine calculus arguments verify that Ω indeed lies inside this trapezoid. To illustrate this, we work out the details for one of the lines, the only one which figures in the proof of Theorem 4.1.

Lemma 4.2 *The region Ω lies beneath the line $t = (2/3)b - (1/2)$.*

Proof: First we check that

$$\frac{\partial g}{\partial t} = 1 + \frac{t}{5 + 5b^2 + t^2} > 0.$$

To finish the proof, it suffices to show that $g > \sqrt{3}$ on our line. The minimum of the function

$$\gamma(b) = g\left(b, \frac{2b}{3} - \frac{1}{2}\right) \tag{11}$$

occurs at $b = (39 + \sqrt{8151})/520$ and the value there is about $\sqrt{3} + .00002$. ♠

One thing we notice right away is $(b, t) \in \Omega$ implies that $b > 0$ and $t < 0$. That is, the bends have opposite slopes. Applying the Intermediate Value Theorem, we get the following result.

Theorem 4.3 *If \mathcal{M} is an immersed paper Moebius band with a T-pattern and aspect ratio less than $\sqrt{3}$ then \mathcal{M} has at least 2 bends of slope 0.*

4.3 Another Constraint

To prove Theorem 4.1 we first establish another constraint imposed by Figure 3.1.

Lemma 4.4 $B^2 - L_j^2 + (T - R_j)^2 \leq 0$ for $j = 1, 2$.

Proof: We take the case $j = 1$. The case $j = 2$ is the same, except that the vector (x, y) is replaced by the vector $(x, -y)$. We set $L = L_1$, etc.

Let

$$\Theta = (B/2 + x, y). \quad (12)$$

The vector (x, y) points from the left endpoint of the horizontal bend image in Figure 3.1 to the midpoint of the vertical bend image. So, Θ points from the midpoint of $I(\beta_b)$ to $I(\beta_t)$.

Let Γ be the portion of the ridge curve corresponding to τ . Here Γ connects $(B, 0, 0)$ to $(0, T, 0)$. Let μ_1, \dots, μ_n be the associated sign sequence. The $(-)$ signs corresponding to the left side of the trapezoid τ and the $(+)$ signs correspond to the right. Let $M_{\pm} \subset \{1, \dots, n\}$ denote those indices i such that $\mu_i = \pm 1$. Let $\Gamma'_1, \dots, \Gamma'_n$ denote the edges of Γ . Let

$$L_{\text{str}} = \sum_{i \in M_-} \Gamma'_i, \quad R_{\text{str}} = \sum_{i \in M_+} \Gamma'_i. \quad (13)$$

It follows from the definitions that

$$\|L_{\text{str}}\| \leq L, \quad \|R_{\text{str}}\| \leq R, \quad R_{\text{str}} + L_{\text{str}} = (-B, T, 0), \quad R_{\text{str}} - L_{\text{str}} = 2\Theta. \quad (14)$$

See Equation 4 for the justification of the last inequality. Define

$$p = (B, 0, 0) + R_{\text{str}} = (0, T, 0) - L_{\text{str}} = \left(\frac{B}{2}, \frac{T}{2}, 0\right) + \Theta. \quad (15)$$

Let π_k be projection onto the k th coordinate. We have $\pi_1(p) = B + x$. Also,

$$\pi_2(p) \leq \|R_{\text{str}}\| \leq R < 1 \leq T.$$

Set $\zeta = (0, T, 0)$. By the Pythagorean Theorem:

$$\|(B, R, 0) - \zeta\| \leq \|(B + x, \|R_{\text{str}}\|, 0) - \zeta\| \leq \|p - \zeta\| = \|L_{\text{str}}\| \leq L. \quad (16)$$

Hence $\|(B, R) - (0, T)\| \leq L$. Squaring both sides and rearranging, we get the advertised constraint. ♠

4.4 Proof of Theorem 4.1

We pick an index $j = 1, 2$ and then set $L = L_j$, etc. Plugging in Equation 8 into the constraint from Lemma 4.4, we see that this constraint is equivalent to

$$2 + b^2 + t^2 + bT - tT - S(b - t + T) \leq 0.$$

Rearranging this expression, we see that we must have

$$S \geq \psi(b, t) := \frac{2 + b^2 + t^2 + bT - tT}{b - t + T}. \quad (17)$$

Hence

$$S + \frac{b(1 - 2b)}{3} - \sqrt{3} \geq \widehat{\psi}(b, t) := \psi(b, t) + \frac{b(1 - 2b)}{3} - \sqrt{3}. \quad (18)$$

Hence, it suffices to prove that $\min_{\Omega} \widehat{\psi} = 0$, where Ω is as in Figure 5.2.

The expression $b - t + T$ is positive when $b \geq t$, which we have on Ω . Using the solvable expression trick on $(b - t + T)\widehat{\psi}$, we find that $\widehat{\psi}(b, t) = 0$ only if $P(b, t) = 0$, where $P(b, t)$ is the following polynomial:

$$4b^6 - 8b^5t - 16b^5 + 20b^4t + 12\sqrt{3}b^4 + 12b^4 - 24\sqrt{3}b^3t - 8b^3t - 24\sqrt{3}b^3 - 8b^3 + 9b^2t^2 + 12b^2t + 30\sqrt{3}b^2t - 12\sqrt{3}b^2 + 59b^2 + 18bt^3 - 42bt - 12\sqrt{3}b + 27t^2 + 18\sqrt{3}t + 9$$

It suffices to prove that $P > 0$ on Ω .

The expression for P is a monster but it is cubic in t . Let Z be the segment which is the subset of the line

$$t = (2/3)b - (1/\sqrt{3}). \quad (19)$$

parametrized by $b \in (0, 1/2)$. Given the description of Ω in Figure 3.1, every point of Ω can be reached from a point of Z by travelling upwards on a vertical ray. So, to prove that $P > 0$ on Ω it suffices to prove that $P''' > 0$ when $b > 0$ and that $P, P', P'' > 0$ on Z . Here we are taking derivatives with respect to t but then we will use Equation 19 to express the answer in terms of b .

We compute $P''' = 108b$, which is certainly positive when $b > 0$. We then compute other derivatives and restrict to Z :

$$P'' = 54 - 36\sqrt{3}b + 90b^2, \quad P' = b(12 + 12b + 28b^2 - 24\sqrt{3}b^2) + b^4(20 - 8b).$$

$$(3/4)P = b^2(21 - 12\sqrt{3} + 18b - 10\sqrt{3}b + 12b^2 - 8\sqrt{3}b^2 - 2b^2) + b^5(2\sqrt{3} - b) \quad (20)$$

On $(0, 1/2)$, every linear polynomial in sight is positive and, as can be checked by the quadratic formula, every quadratic polynomial is positive as well. Hence, the expressions in Equation 20 are all positive on $(0, 1/2)$. This completes the proof.

5 A Big Calculation

5.1 Tensegrities

To put the big calculation in perspective, we give a brief discussion of tensegrities. Roughly, a *tensegrity* is a metric graph with 2 kinds of edges, “wooden” edges and “elastic” edges. A realization of the tensegrity is a straight line embedding of the graph in space which is length-preserving along the wooden edges and length-non-increasing along the elastic edges. There are many variants of this basic definition considered in the literature. See [CB] and the references therein for a survey on tensegrities. A paper Moebius band behaves somewhat like a tensegrity, because the embedding is an isometry along the bend lines and a weak contraction in the transverse directions.

One can view the trapezoids in Figure 3.1 as finite tensegrities which very crudely approximate the paper Moebius band. In a sense, all our estimates above derive from this approximation. We can get more information by taking a finer approximation. Concretely, this amounts to taking (say) the lower trapezoid in Figure 3.1 and inserting another bend, which we call m . Figure 5.1 illustrates this.

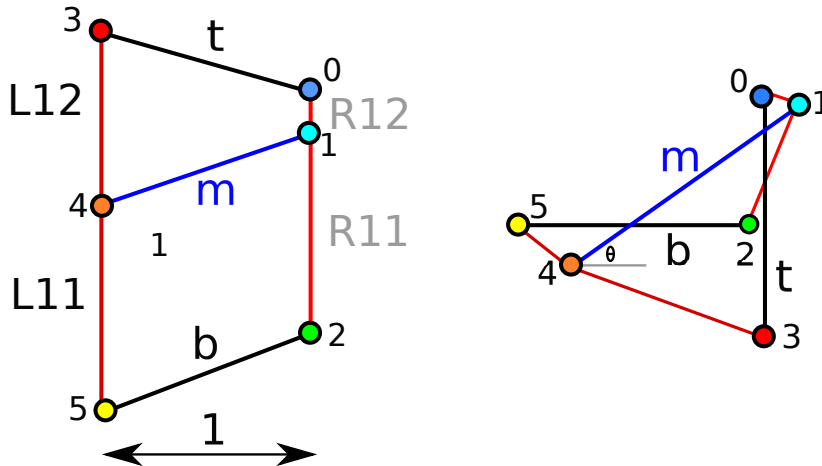


Figure 5.1: A finer picture

Comparing Figure 5.1 to Figure 3.1, we have

$$L_1 = L_{11} + L_{12}, \quad R_1 = R_{11} + R_{12}.$$

The bend image labeled m on the right does not necessarily lie in the XY -plane – i.e., the plane containing the T -pattern – but we are showing a projection into this plane. The angle θ is the angle that the projection that this bend image makes with the X -axis. We will be most interested in the case when $\theta = \pi/6$, as is approximately shown in the picture.

5.2 The Capacity

Let Υ denote the figure on the left side of Figure 5.1 and let Υ^* denote the figure on the right. Υ is parameterized by 5 numbers $(m, b, t, L_{11}, L_{12})$. Here b, m, t are respectively the slopes of the bottom, middle, and top segments. We have

$$R_{11} = L_{11} - b + m, \quad R_{12} = L_{12} - m + t, \quad (21)$$

Let v_0, \dots, v_5 be the 6 vertices on the left.

The right side Υ^* consists of 3 segments labeled b, m, t . We will discuss its parameterization below. Let v_0^*, \dots, v_5^* be the corresponding vertices. We call (Υ, Υ^*) a *tensegrity pair* if $\|v_i - v_j\| \geq \|v_i^* - v_j^*\|$ for all pairs of indices connected by edges, and furthermore that $\|v_i - v_j\| = \|v_i^* - v_j^*\|$ for the specific pairs

$$(i, j) = (0, 3), (1, 4), (2, 5).$$

These correspond to the bends. The three edges corresponding to the special pairs are the wooden edges and the remaining edges are elastic. Any immersed paper Moebius band with a T -pattern gives rise to a tensegrity pair.

We let

$$S(\Upsilon) = L_{11} + L_{12} + R_{11} + R_{12}. \quad (22)$$

If we can prove that $S(\Upsilon) > \lambda_2$ for all Υ^* participating in a tensegrity pair, then we have proved that any immersed paper Moebius band with a T -pattern has aspect ratio at least λ_2 .

Let us be systematic about this. We can fix the right half Υ^* and vary the left half. We define the *capacity* of Υ^* to be the minimum of $S(\Psi)$, taken over Ψ such that (Ψ, Υ^*) is a tensegrity pair. We can compute the capacity of Υ^* in an easy way. We define

$$L_{11} = \max(d_{45}^*, d_{12}^* + b - m), \quad L_{12} = \max(d_{34}^*, d_{01}^* + m - t). \quad (23)$$

We then define R_{11} and R_{12} using Equation 21.

Let $C(\theta)$ denote the minimum capacity, taken over all right hand configurations with angle θ . If we have some bound like $C(\theta) > \lambda_2$ then it immediately tells us that an immersed paper Moebius band with a T -pattern has aspect ratio at least λ_2 .

We played around with various choices of θ and we found, at least numerically, that

$$C(\pi/6) > \sqrt{3} - .017 > \sqrt{3} - (1/58).$$

We put the final estimate so as to compare it more easily with our other results. Other values of θ seem to give weaker bounds. For instance, $C(\pi/3) < \sqrt{3} - .03$. We also note that it is possible to strengthen the notion of capacity by adding in more edges. For instance, we could also demand that $d_{15} \geq d_{15}^*$. This turns out not to improve the calculation of $C(\pi/6)$.

5.3 The Calculation

Now we describe, in brief, how our numerical experiments work. Up to isometry, the space of configurations like Υ^* , with fixed value of θ , is 9-dimensional. Call a set of such configurations *ample* if it contains all the configurations having capacity less than $\sqrt{3}$. We can parametrize an ample subset by the unit cube $[0, 1]^9$. For instance, the first two coordinates pick out a point in the parallelogram bounded by the conditions

$$b \in [0, 1/2], \quad t - (2/3)b \in [-1/2, -1/\sqrt{3}].$$

This specifies the slopes b and t in a way that is guaranteed to cover the set Ω from Figure 4.1. In our calculations we made some reasonable choices which do not seem worth discussing here in detail.

We get an experimental bound on $C(\pi/6)$ as follows. We start with a random point in $[0, 1]^9$ and compute the capacity. We then pick a nearby point at random and recompute. If the capacity is lower, we move to the new point. Now we iterate. I believe that this is called a *hill-climbing algorithm*. We leave the program running all night and check in the morning. Of course, this method gives no guarantee that we are finding the actual minimum.

Were this calculation rigorous and exhaustive, it would improve the bound in Theorem 1.1 to $\sqrt{3} - 0.017$. One could try to make this calculation rigorous along the lines of, say, my paper on Thomson's 5-electron problem [S2]. The calculation there involved a 7-dimensional configuration space, which comparatively speaking is a walk in the park. The basic idea is to establish an *a priori* estimate which bounds the capacity of any configuration in some product subset $Q \subset [0, 1]^9$ using finitely many calculations. For instance, we could compute the capacity of the configuration corresponding to the center of mass of Q , and then subtract off a bound larger than the Lipschitz constant of the capacity function multiplied by the radius of Q . We could then use a divide and conquer algorithm, a depth-first-search through the poset of dyadic product subsets, to establish an inequality like the kind mentioned above.

The kind of tensegrity calculation mentioned above is just the tip of the iceberg. I did many experiments like this. As another example, if tensegrity on the right side of Figure 5.1, with $\theta = \pi/12$, has capacity less than $\sqrt{3} - \epsilon$, it seems that the vertex v_1^* sticks out at least $(\sqrt{3}/2)\epsilon$ beyond the edge $\overline{v_0^*v_2^*}$. The other half of the paper Moebius band would then have to go around this "bump", giving it too much length to have aspect ratio less than $\sqrt{3}$. In reality, there are many steps needed to rigorously make such a deduction, but I had hoped that considerations like this would establish that $\lambda_0 = \sqrt{3}$. Alas, I have not yet been able to make these tensegrity calculations feasible.

6 References

- [**AHLM**] A. Malaga, S. Lelievre, E. Harriss, P. Arnoux,
ICERM website: <https://im.icerm.brown.edu/portfolio/paper-flat-tori/> (2019)
- [**CB**], R. Connolly, A Back, *Mathematics and Tensegrity*, in **American Scientist**, Vol 82 **2**, (March-April 1998) pp 142-151.
- [**CF**] Y. Chen and E. Fried, *Mobius bands, unstretchable material sheets and developable surfaces*, Proceedings of the Royal Society A, (2016)
- [**CKS**] J. Cantarella, R. Kusner, J. Sullivan, *On the minimum ropelength of knots and links*, Invent. Math. **150** (2) pp 257-286 (2003)
- [**FT**], D. Fuchs, S. Tabachnikov, *Mathematical Omnibus: Thirty Lectures on Classic Mathematics*, AMS 2007
- [**HF**, D.F. Hinz, E. Fried, *Translation of Michael Sadowskys paper An elementary proof for the existence of a developable MBIUS band and the attribution of the geometric problem to a variational problem*. J. Elast. 119, 36 (2015)
- [**HW**], B. Halpern and C. Weaver, *Inverting a cylinder through isometric immersions and embeddings*, Trans. Am. Math. Soc **230**, pp 41.70 (1977)
- [**MK**] L. Mahadevan and J. B. Keller, *The shape of a Mobius band*, Proceedings of the Royal Society A (1993)
- [**Sa**], M. Sadowski, *Ein elementarer Beweis fr die Existenz eines abwickelbaren MBIUSschen Bandes und die Zurckfhrung des geometrischen Problems auf ein Variationsproblem*. Sitzungsberichte der Preussischen Akad. der Wissenschaften, physikalisch-mathematische Klasse 22, 412415.2 (1930)
- [**S1**] G. Schwarz, *A pretender to the title “canonical Moebius strip”*, Pacific J. of Math., **143** (1) pp. 195-200, (1990)
- [**S2**] R. E. Schwartz, *The 5 Electron Case of Thomson’s Problem*, Journal of Experimental Math, 2013.
- [**W**] S. Wolfram, *The Mathematica Book, 4th Edition*, Wolfram Media and Cambridge University Press (1999).